Plant Physiology Preview. Published on October 21, 2016, as DOI:10.1104/pp.16.01347

Short title: Cell-specific mechanisms of salt tolerance in barley

Corresponding author: Prof Sergey Shabala
School of Land and Food, University of Tasmania, Private Bag 54, Hobart, Tas 7001, Australia. Email**:** Sergey.Shabala@utas.edu.au; Phone +61362267539

Cell-type specific H^+-ATPase activity in root tissues enables K^+ retention and mediates acclimation of barley (*Hordeum vulgare* L.) to salinity stress[1]

Lana Shabala[1], Jingyi Zhang[1], Igor Pottosin[1,2], Jayakumar Bose[1,3], Min Zhu[1], Anja Thoe Fuglsang[4], Ana Velarde-Buendia[2], Amandine Massart[5], Camilla Beate Hill[6], Ute Roessner[6], Antony Bacic[7], Honghong Wu[1], Elisa Azzarello[8], Camilla Pandolfi[8], Meixue Zhou[1], Charlotte Poschenrieder[5], Stefano Mancuso[8], and Sergey Shabala[1,2]

[1]School of Land and Food, University of Tasmania, Hobart, Tas 7001, Australia; [2]Centro Universitario de Investigaciones Biomédicas, Universidad de Colima, Colima, 28045, México; [3]ARC Centre of Excellence in Plant Energy Biology and School of Agriculture, Food and Wine, University of Adelaide, Glen Osmond, SA 5064, Australia; [4]Department of Plant and Environmental Sciences, University of Copenhagen, DK-1871, Denmark; [5]Fisiología Vegetal, Facultad de Biociencias, Universidad Autónoma de Barcelona, Bellaterra, Spain; [6]School of BioSciences, University of Melbourne, Vic 3010, Australia; [7]ARC Centre of Excellence in Plant Cell Walls, School of BioSciences, University of Melbourne, Vic 3010, Australia; [8]Department of Horticulture, University of Florence, 50019, Italy

One sentence summary:

The differential sensitivity of various root tissues to salt stress is not related to their ability to exclude or sequester sodium but rather is determined by the differences in their ability to retain potassium.

[1] This work was supported by separate grants from the Australian Research Council and Grain Research and Development Corporation to SS, AB (CE1101007), CBH and UR.

[2] Corresponding author. Email: Sergey.Shabala@utas.edu.au

ABSTRACT

While the importance of cell-type specificity in plant adaptive responses is widely accepted, only a limited number of studies have addressed this issue at the functional level. We have combined electrophysiological, imaging, and biochemical techniques to reveal physiological mechanisms conferring higher sensitivity of apical root cells to salinity in barley. We show that salinity application to the root apex arrests root growth in a highly tissue- and treatment-specific manner. Although salinity-induced transient net Na^+ uptake was about 4-fold higher in the root apex compared with the mature zone, mature root cells accumulated more cytosolic and vacuolar Na^+ suggesting that higher sensitivity of apical cells to salt is not related to either enhanced Na^+ exclusion or sequestration inside the root. Rather, the above differential sensitivity between the two zones originates from a 10-fold difference in K^+ efflux between the mature zone and the apical region (much poorer in the root apex) of the root. Major factors contributing to this poor K^+ retention ability are: (1) an intrinsically lower H^+-ATPase activity in the root apex; (2) greater salt-induced membrane depolarization and (3) a higher ROS production under NaCl and a larger density of ROS-activated cation currents in the apex. Salinity treatment increased (2 to 5 fold) the content of 10 (out of 25 detected) amino acids in the root apex but not in the mature zone and changed the organic acid and sugar contents. The causal link between observed changes in the root metabolic profile and regulation of transporters activity is discussed.

Key words: ion flux; membrane potential; oxidative stress; potassium; H^+-ATPase; sodium sequestration; salinity

INTRODUCTION

Soil salinity is a major environmental constraint to crop production that affects about 20% of irrigated land costing US$ 27.3 billion p.a. in lost revenue (Qadir et al., 2014). To date attempts to create salt-tolerant crop germplasm have had limited success (Flowers, 2004; Shabala, 2013), largely due to the high physiological and genetic complexity of this trait. It is estimated that salinity affects transcripts of approximately 8% of all genes (Tester and Davenport, 2003), and fewer than 25% of these salt-regulated genes are salt stress-specific (Ma et al., 2006). At the physiological level, numerous sub-traits contribute to overall salinity tolerance, most of which are species-specific and may require expression in either a particular tissue- or cell-type (Tester and Davenport, 2003; Shabala, 2013). It is thought that the limited

61 success of transgenic manipulations to increase some of these traits (and, specifically, those
62 related to ion exclusion from the shoot) is largely due to the inability to express important
63 exclusion genes in a cell-specific manner (Roy et al., 2014).

64 While the importance of cell-specific responses for plant adaptive responses to the
65 environment is widely accepted (Ma and Bohnert, 2007; Dinneny et al., 2008; Dinneny,
66 2010), only a limited number of studies have attempted to address this issue in respect to salt
67 stress. Dinneny et al. (2008) used fluorescence-activated cell sorting to generate a genome-
68 scale high-resolution expression map to demonstrate cell-type specific responses of various
69 root cell types to salinity. Several thousand genes were shown to be expressed in a cell-
70 specific manner, both in terms of longitudinal and radial root profiles (Dinneny et al., 2008).
71 Although highlighting the complexity of plant adaptive responses to salinity, these results
72 cannot be easily translated into breeding programs. Transcriptional changes do not necessarily
73 reflect physiological changes (Adem et al., 2014) and, thus, should be interpreted with some
74 caution. The same notion is applicable to other techniques used to reveal tissue-specific
75 patterning of transporter expression. For example, using a GFP fusion technique the
76 preferential expression of SOS1 (salt overly sensitive) Na^+/H^+ exchanger was reported for the
77 epidermal cells of the root tip and xylem/symplast boundary (Shi et al., 2000, 2002). Yet, the
78 functional analysis of Arabidopsis *sos1* transport mutants has revealed significant differences
79 in root K^+ retention ability between *sos1* and wild type plants in the mature root epidermis
80 (Shabala et al., 2005), where no GFP signals were detected (Shi et al., 2000). At the same
81 time, it is the function of the specific transporter/protein that ultimately determines plant
82 adaptive responses to salinity. Therefore, there is a need to address the issue of tissue- and
83 cell-specificity of salt responses at the functional level.

84 Physiologically, plant adaptive responses to salinity can be grouped into four major
85 categories: (1) dealing with the osmotic component of salt stress; (2) handling toxic Na^+ and
86 Cl^- ions; (3) detoxifying reactive oxygen species (ROS) produced in plant tissues under saline
87 conditions; and (4) mediating cytosolic K^+ homeostasis (Tester and Davenport 2003; Ji et al.,
88 2013; Shabala, 2013; Shabala and Pottosin, 2014; Julkowska and Testerink, 2015; Kurusu et
89 al., 2015; Flowers et al., 2015). All these responses rely heavily on regulation of transport
90 activity across cellular membranes and, specifically, those for Na^+ and K^+ ions. High
91 cytosolic Na^+ concentrations are considered to be toxic for cell metabolism and, thus, are
92 reduced by various means (Tester and Davenport, 2003; Ji et al., 2013; Flowers et al., 2015).
93 At the same time, superior K^+ retention and a cell's ability to maintain cytosolic K^+

homeostasis correlates with salinity tolerance in a broad range of plant species (Shabala and Pottosin, 2014; Anschutz et al., 2014) and is essential for preventing salinity-induced programmed cell death (Shabala, 2009; Demidchik et al., 2010). High cytosolic K^+ levels are also essential to maintain high vacuolar H^+-PPase activity thus enabling operation of tonoplast NHX proteins that mediate vacuolar Na^+ sequestration (Shabala, 2013). Na^+ and K^+ are also major inorganic osmolytes that confer over 70 % of tissue osmotic adjustment under stress conditions (Shabala and Lew, 2002). In addition, ROS detoxification activity in plant cells is critically dependent on K^+ availability (Sun et al., 2015). This explains why the cytosolic Na/K ratio is widely regarded a major determinant of plant salinity stress tolerance (Shabala and Pottosin, 2014; Anschutz et al., 2014) and why understanding the tissue-specificity of its regulation may be the key to improving salinity tolerance in plants.

In this work, we address some of above gaps in our knowledge and provide a comprehensive characterization of the functional activity of the major transport systems conferring Na^+ and K^+ ionic relations in salinized plant tissues, at the cell-specific level and then link it to the stress-induced changes in the tissue metabolic profile. Using barley roots as a model system we show that compromised K^+ retention in the root is the main detrimental factor that contributes to barley's tolerance to salinity. We show that root apical cells are much more sensitive to salt stress, and attribute this differential sensitivity to superior K^+ retention in mature root epidermis originating from intrinsically higher H^+-ATPase activity (and, hence, the ability to maintain more negative membrane potential) and reduced sensitivity of Na^+- and K^+-permeable NSCC to ROS generated under saline conditions.

RESULTS

Root growth is arrested in a stress-specific manner following the administration of NaCl to the root apex but not the mature root zone

We designed a multi-compartment chamber that allows for the application of different treatments to specific root zones (Suppl. Fig 1; Fig 1A). Compartments I to III covered the major bulk of the mature root zone, and compartment IV was covering elongation and meristematic root zones (root apex; Fig 1B). For roots grown under control conditions, all four compartments were filled with BSM solution. For stress treatment, BSM solution in either compartments II (mature zone) or IV (root apex) was replaced by either 100 mM NaCl or isotonic 170 mM mannitol solution. The roots were immobilized such that in each zone of the root the same surface area was exposed to the treatment (a 4 mm-long segment; Fig 1A).

Exposure of the root apex (the first 4 mm of the root from the tip) to 100 mM NaCl resulted in an immediate arrest of the root growth (Fig 1C, D). The same treatment applied to the mature root zone (root segment between 14 and 18 mm from the tip) did not result in any significant ($P<0.05$) decline in root growth compared with controls over the 3 day period of the experiment (Fig 1C, D). Impaired root growth was salt stress-specific as it was not observed when roots were treated with isotonic mannitol (Fig. 1C, D). Both treatments resulted in significant accumulation of Na^+ and loss of K^+ from exposed roots ($P<0.05$; Fig 1E). While Na^+ accumulation was independent of the zone of salt application, roots treated with 100 mM NaCl in the apical region lost more K^+ compared with those treated in the mature zone ($P<0.05$; Fig 1E). This difference could not be attributed to the potential "dilution effect" in growing roots, as higher K^+ content was measured in the bulk of the roots still undergoing growth (where salt treatment was applied to a part of mature zone; a blue bar in Fig 1E) but not the roots with arrested growth (apical treatment; a green bar in Fig 1E). Thus, the "dilution effect" (if any) may only lead to the potential underestimation of the difference in K^+ uptake or retention ability between two zones.

The reported differences in ion accumulation are not related to the differences in root lignification between these two regions (data not shown), and such K^+ loss was not observed in mannitol-treated roots (data not shown). Taken together, the results suggest that (i) root apical tissues are much more sensitive to salinity and are immediately growth arrested upon salinity treatment; (ii) the above effect is salt stress-specific and may be related to a differential ability of root tissues to retain K^+, rather than restrict Na^+ uptake.

Fig 1

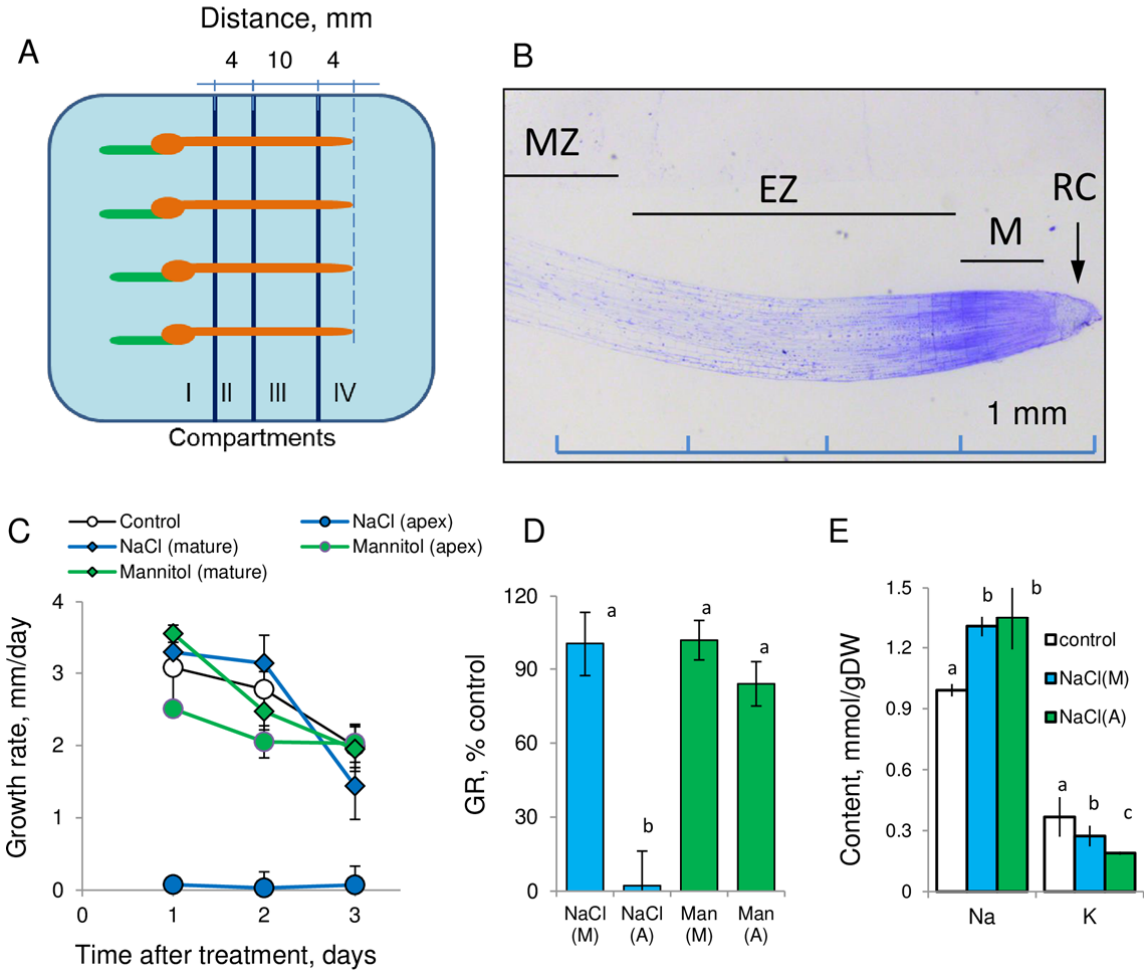

Fig 1: Barley root growth and responses to salinity (100 mM NaCl) and isotonic mannitol treatment. **A** – A schematic diagram depicting the experimental design and root immobilization within a multi-compartment growth chamber (see Suppl Fig 1). Salt was added to compartments II (mature zone) and IV (root apex), respectively. **B** – anatomy of barley root apex depicting functionally different root zones (modified from Ryan et al., 2016 with permission from Oxford University Press). RC – root cap; M – meristem; EZ – elongation zone; MZ – mature zone. **C** - Root growth rate as a function of time after treatment. Mean ± SE (n = 8 to 12). **D** – Relative growth rate (GR; % of control); **E** – total root Na^+ and K^+ content after 3 days of 100 mM NaCl application to either apical or mature root zones. Mean ± SE (n = 5 to 8). Man, mannitol; (M), mature zone; (A), apex. Different lowercase letters indicate significant differences between treatments at $P < 0.05$.

Differential sensitivity in growth responses is not related to higher Na^+ accumulation in the root apex

Upon acute NaCl stress, salinity-induced net Na^+ uptake was about 4-fold higher in the root apex compared with the mature zone (Fig 2A). However, this difference was transient, lasting less than 10 min, with fluxes gradually reducing to near-zero levels. Confocal imaging using CoroNa Green fluorescent dye revealed that despite net Na^+ uptake being higher in the root

Fig 2

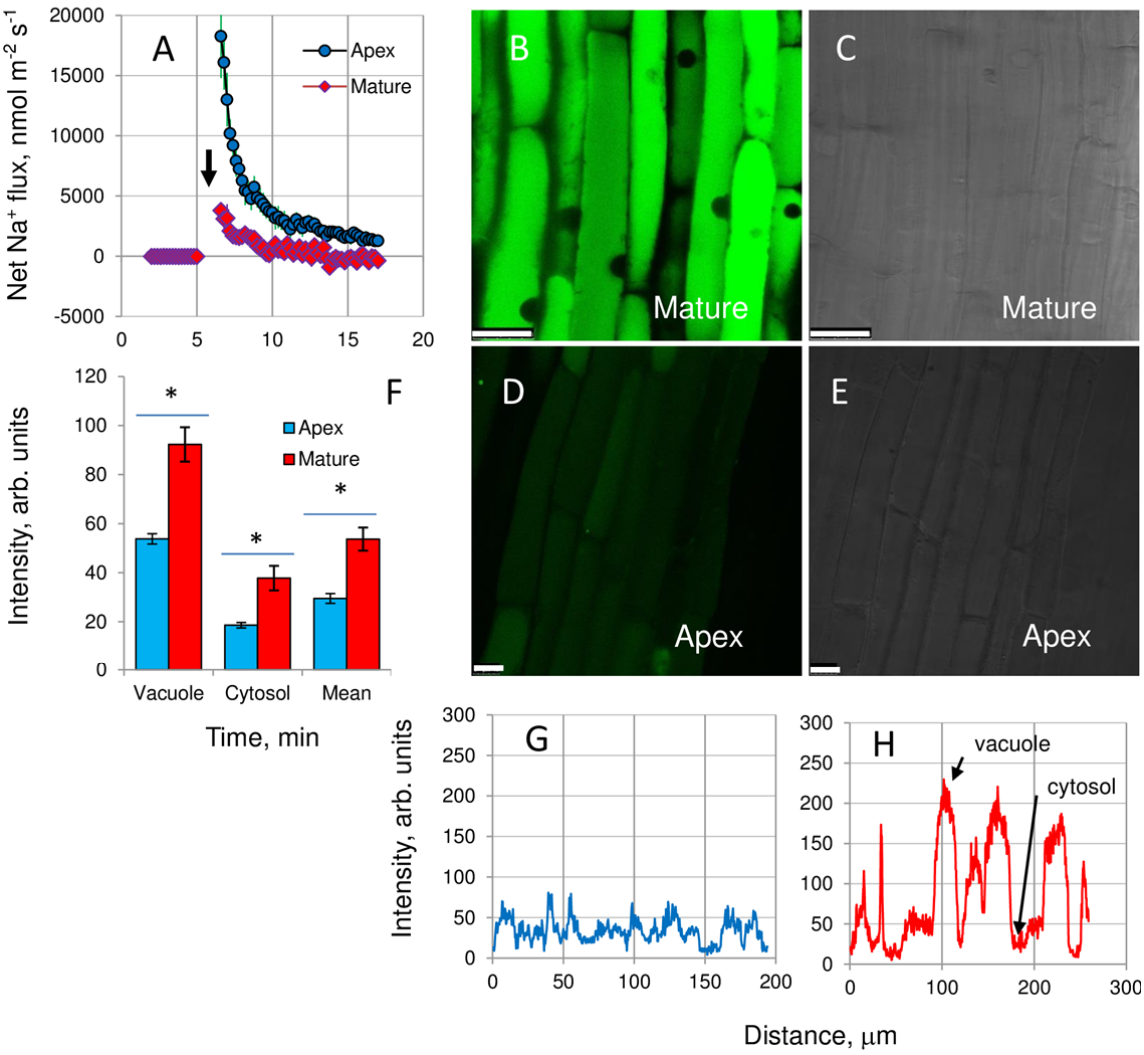

Fig 2: Na^+ uptake and accumulation in barley roots. **A** – kinetics of net Na^+ fluxes measured from the epidermal root cells in the apical and mature regions in response to 100 mM NaCl treatment (indicated by an arrow). Mean ± SE (n = 6 to 8). **B, D**– Na^+ accumulation and intracellular distribution in mature (**B**) and apical (**D**) root zones visualized by the CoroNa Green fluorescence dye after 3 days of 100 mM NaCl treatment. One (of 8) typical image for each zone is shown. All images were taken using the same settings and exposure times to enable direct comparisons. Panels **C** and **E** show bright-field images of the corresponding zones for **B** and **D**, respectively. **F** – Mean CoroNa Green fluorescence intensity measured from cytosolic and vacuolar compartments. Mean ± SE (n = 70 to 300). Asterisk indicates significant differences between zones at $P < 0.05$. **G, H** – typical examples of the spatial cross-sectional profiles of CoroNa Green fluorescent signals from roots in apical and mature root zones, respectively. Several lines have been drawn across the so-called "region of interest" (ROI) in an appropriate root zone and continuous fluorescence intensity distribution profiles were obtained by LAS software and plotted. The scale bar in **B-D** is 25 μm.

apex upon stress onset, mature root cells accumulated more Na^+ (Fig 2B-H) compared to apical cells when exposed to prolonged (3 days) salinity treatments. The intensity of the fluorescence signal was much brighter in mature (Fig 2B) compared with apical (Fig 2D) root zones. In quantitative terms, a two-fold higher fluorescent signal was measured from both

160 vacuolar and cytosolic compartments in mature root zone compared with apical cells (Fig 2F;
161 significant at $P < 0.05$). Thus, the arrest of the root growth upon exposure of the apical tissue
162 to salt (see Fig 1) cannot be explained by an accumulation of Na^+ in the root apex. Also, the
163 ratio of fluorescence dye intensity between the vacuolar and cytosolic compartments was very
164 similar for both apical and mature tissue (2.89 ± 0.24 vs 2.45 ± 0.19; not significant at $P <$
165 0.05), suggesting no difference in vacuolar Na^+ sequestration ability.
166
167 ***Apical cells have lower H^+-pumping ability, are more depolarized, and retain less K^+ when***
168 ***exposed to salinity***
169 Salinity treatment resulted in a significant membrane depolarization of epidermal cells (by 74
170 ± 2 mV; Fig 3A). The intrinsic (steady-state) membrane potential (MP) values of mature cells
171 in control were much more negative compared with apex cells (-128 ± 3.9 mV vs -111 ± 3.1
172 mV, respectively; $P < 0.01$; Fig 3A). Also, cells in the mature zone showed higher potency for
173 repolarization. As a result, the new steady-state MP values under saline conditions were
174 nearly 40 mV more negative in the mature zone (-96 ± 2.3 mV vs -58 ± 1.8 mV, respectively;
175 $P < 0.01$; Fig 3A). Physiologically, this difference in steady-state values is critical to
176 determining plant ionic balance and was expected to be reflected in the cell's ability to retain
177 K^+ by either controlling depolarization-activated outward-rectifying (GORK in Arabidopsis)
178 K^+ channels (Very et al., 2014) or any non-selective cation channel, active at depolarized
179 potentials (Demidchik and Maathuis, 2007). Indeed, while a substantive peak K^+ efflux of ~
180 2,100 nmol m^{-2} s^{-1} was measured from the root apex in response to 100 mM NaCl treatment
181 (Fig 3B), this efflux was only ~ 80 nmol m^{-2} s^{-1} in cells in the mature zone. Furthermore, the
182 steady-state fluxes before and after salinity treatment were significantly ($P<0.01$) different,
183 with a 7.5-fold difference in net K^+ flux reported between the two zones 20 min after NaCl
184 application (-600 ± 116 vs -80 ± 32 nmol m^{-2} s^{-1}, respectively; Fig 3B; significant at $P < 0.01$).
185 This may explain the difference in the overall root K^+ content between treatments reported in
186 growth experiments (Fig 1E).

187 The plasma membrane (PM) H^+-ATPase is known to be a major determinant of MP
188 (Palmgren and Nissen, 2011) and more negative MP values in mature root zones could thus
189 be a direct consequence of a more active H^+ pump. To test this, PM vesicles were purified
190 from the root apex and mature zone of control- and salt-grown plants, followed by an H^+-

Fig 3

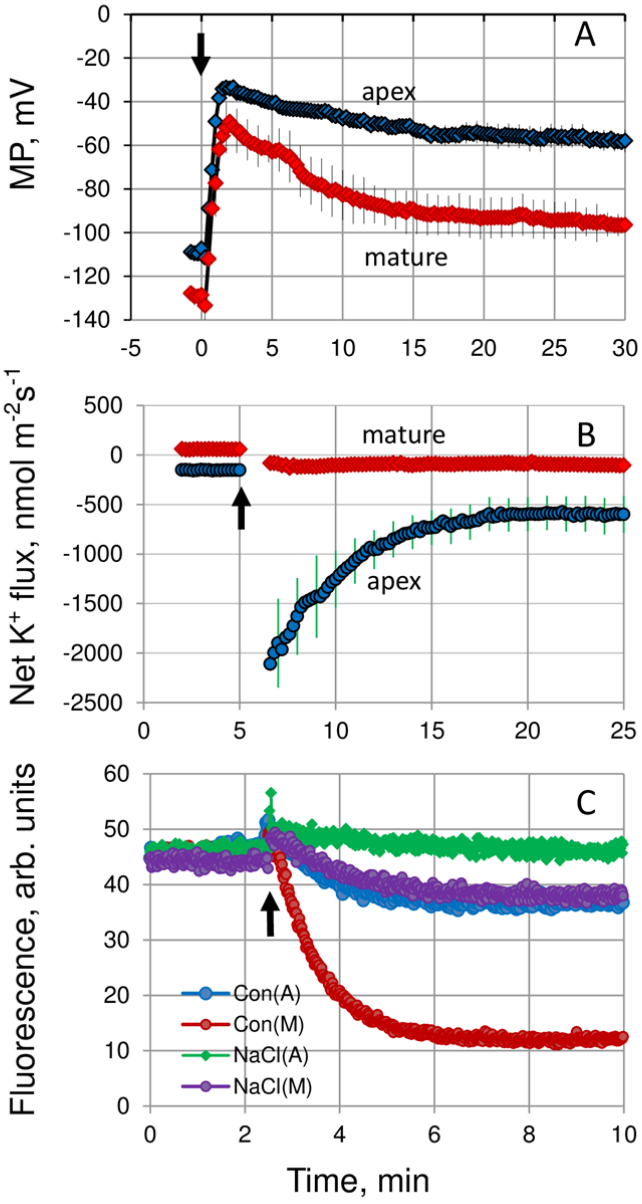

Fig 3: Superior K^+ retention in the mature root zone is attributed to an intrinsically higher rate of H^+-ATPase extrusion activity. **A** – Changes in the PM potential in epidermal root cells in two different zones upon exposure to 100 mM NaCl. Mean ± SE (n = 6 to 8). **B** – Net K^+ fluxes measured from the epidermal root cells in the apical and mature zones in response to 100 mM NaCl treatment (indicated by an arrow). Mean ± SE (n = 7 to 10). **C**- H^+ pumping measured by ACMA quenching. PMs containing the H^+-ATPase were incubated with ATP, and H^+ pumping was activated by addition of Mg^{2+} (indicated by an arrow). The experiment is a representative of three independent PM purifications.

ATPase activity assay using a fluorescent ACMA probe. ACMA accumulates in an impermeable form inside vesicles upon protonation, with a decrease in fluorescence directly correlated to the amount of H^+ transported into the vesicles. Cells in the mature zone

194 exhibited a higher H^+ pumping capacity compared to apex cells as indicated by the slope of
195 curve after H^+-ATPase activation by Mg^{2+} (Fig 3C). Salinity treatment decreased the H^+-
196 ATPase activity in both zones, however, the H^+-ATPase activity was much higher in the
197 mature zone (Fig 3C). Taken together, we conclude that the higher sensitivity of the root apex
198 to salinity is related to its poor K^+ retention ability which originates from a lower H^+-ATPase
199 activity and, hence, inability to maintain a sufficiently negative MP.
200
201 ***Higher sensitivity of the root apex to salinity may be related to a higher ROS accumulation***
202 ***and a larger density of ROS- activated cation current***
203 Salinity stress results in a rapid production of ROS (Mittler 2002). Indeed, root treatment with
204 100 mM NaCl resulted in significant accumulation of ROS in barley roots (Fig. 4). However,
205 this salt-induced accumulation was highly tissue-specific and observed only in the root apex
206 (Fig 4A, B, E) and, specifically, in the elongation zone (see Fig 1B). In contrast, a decrease of
207 fluorescence was observed in the mature root zone under salt stress (Fig 4 C, D, E). While the
208 salt-induced increase in ROS accumulation in the apical zone was NaCl-specific and was not
209 observed in roots exposed to isotonic sorbitol treatment (Fig 4F), the quenching of the
210 fluorescence in the mature root zones was non-specific i.e. activated by both NaCl and
211 sorbitol (Fig 4E, F).
212 This accumulation of ROS in the elongation zone of salinized roots may have major
213 implications for the intracellular ionic homeostasis. By interacting with transition metals such
214 as either Cu or Fe, increased accumulation of H_2O_2 may result in a formation of highly
215 reactive hydroxyl radicals ($OH^{\bullet}$), both in the apoplast (Demidchik, 2015) and cytosol
216 (Rodrigo-Moreno et al., 2013). Both H_2O_2 and $OH^{\bullet}$ may cause a major perturbation in
217 intracellular ionic homeostasis by activating a range of cation-permeable ion channels
218 (Demidchik and Maathuis, 2007; Demidchik et al., 2010; Shabala and Pottosin, 2014). Thus,
219 tissue-specific salinity stress sensitivity between the root apex and mature zones may be
220 causally related to the patterns of $OH^{\bullet}$ production and/or sensitivity of membrane transporters
221 to $OH^{\bullet}$. Consistent with this hypothesis, the application of $OH^{\bullet}$-generating Cu/ascorbate mix
222 resulted in a rapid and substantive Ca^{2+} uptake and K^+ efflux from barley roots (Fig. 5). Both
223 responses were an order of magnitude higher in the root apex compared with mature root
224 zone. This suggests that increased production of ROS, which is able to induce greater K^+ loss
225 from the root apex as compared to the mature zone, may be the cause of the higher salt
226 sensitivity of the former tissue.

Fig 4

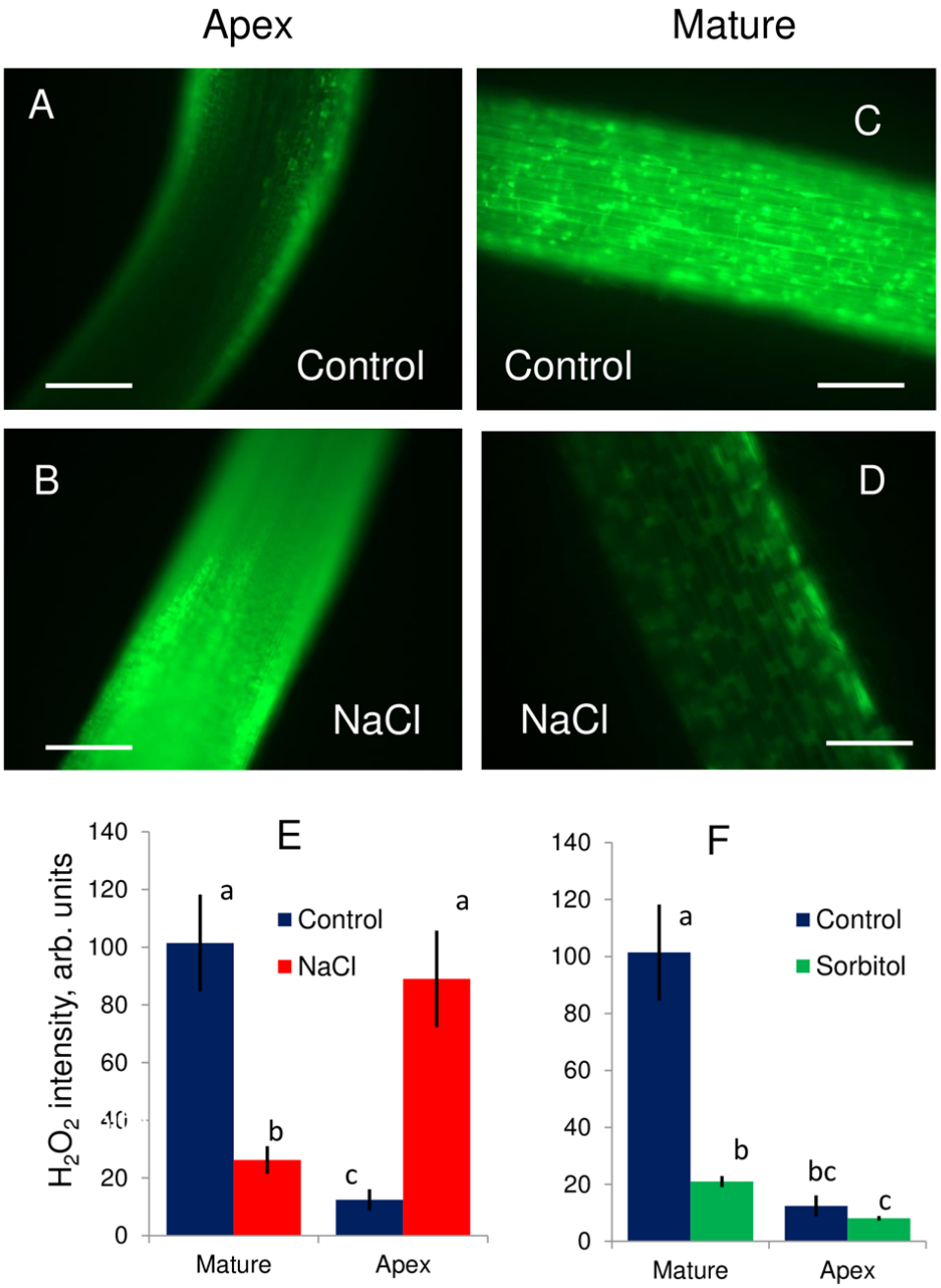

Fig 4: Stress-induced ROS accumulation in barley roots visualised by 2', 7' Dichlorofluorescein diacetate (DCF-DA) staining (see Rodrigo-Moreno et al., 2013 for details). Panels **A- D** show representative (one of eight) images of mature (~20 mm from tip) and apical (2 mm) zones from control and salt-treated (100 mM NaCl for 24 h) roots. **E** - average fluorescence signal intensity from the midst of the apical and mature root zone (in arbitrary units) for control and stressed roots. Mean ± SE (n = 8). F – as above, for root treated with isotonic mannitol solution. Data labelled with different lower case letters is significantly different at $P < 0.05$. The scale bar in panels **A-D** is 200 µm.

227 To elucidate the nature of membrane transporters mediating these pronounced K^+ and
228 Ca^{2+} fluxes, we conducted a series of patch-clamp experiments, targeting $OH^{\bullet}$ -induced
229 currents, known to confer K^+ and Ca^{2+} transport across the root PM. Consistent with previous

Fig 5

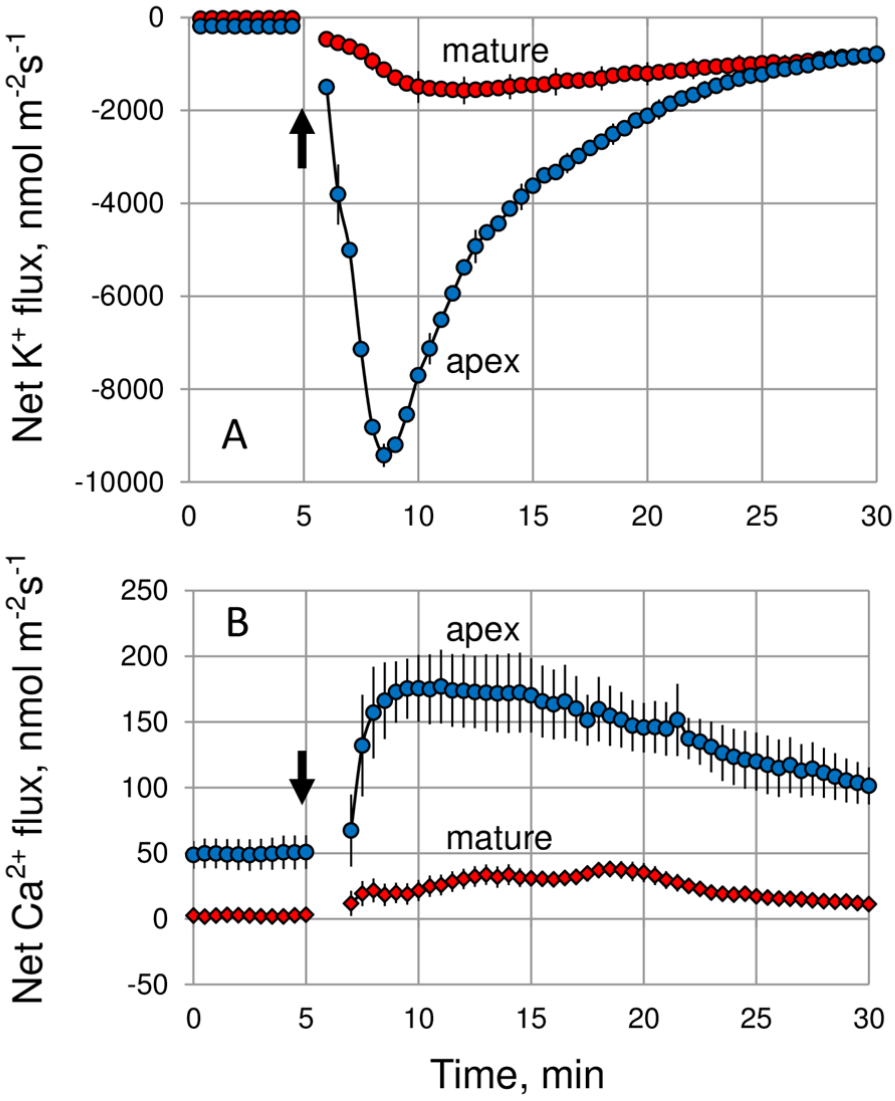

Fig 5: Net K^+ (**A**) and Ca^{2+} (**B**) fluxes measured from epidermal root cells in response to $OH^{\bullet}$-generating Cu/ascorbate (0.3/1 mM) mix applied at 5 min (as indicated by an arrow). Mean ± SE (n = 6 to 8).

observations, the $OH^{\bullet}$ -induced current was biphasic composed of the instantaneous and the time-dependent depolarization-activated components (Fig. 6A), which could be tentatively assigned to ROS-activated NSCC and GORK, respectively (Demidchik et al., 2014; Shabala and Pottosin, 2014). Due to a strong outward rectification, a reversal potential of the time-

Fig 6

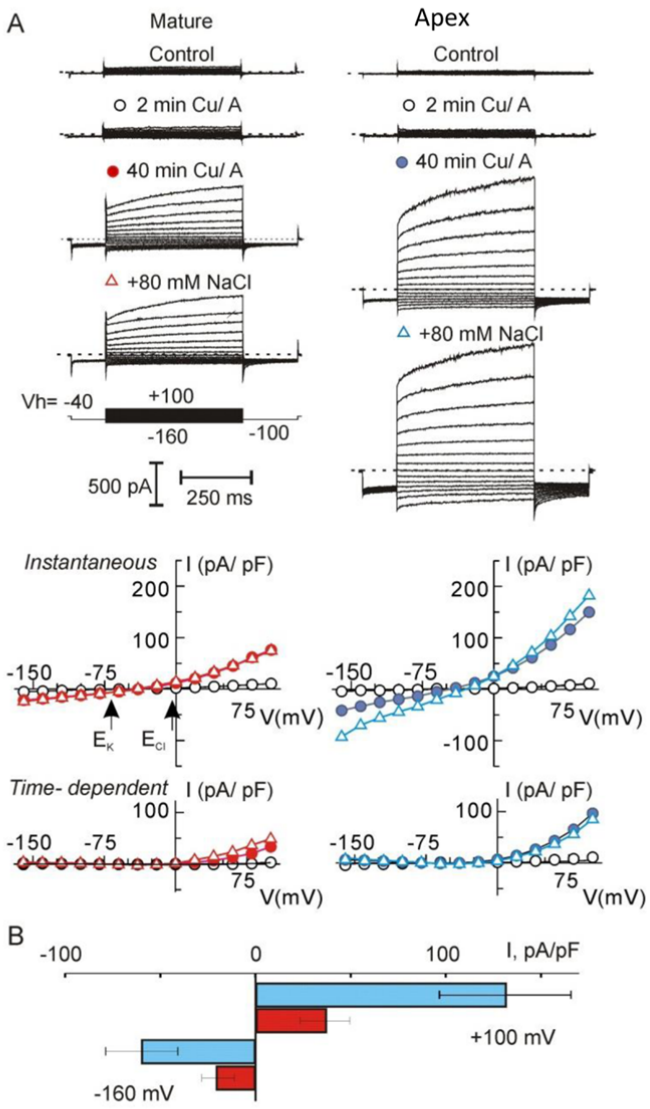

Fig 6: ROS induced non-selective current in protoplasts from elongation and mature root zones. (**A**) Examples of whole cell recordings of membrane currents, induced by OH• in two protoplasts of equal size (C=5.5 pF), isolated from mature or elongation root zones. Ionic concentrations are given in Materials and Methods. Respective I/V curves for instantaneous and time-dependent current components at the beginning of treatment (2 min), 40 min after, and after a subsequent addition of 80 mM NaCl are presented. Arrows indicate equilibrium potentials for K^+ and Cl^- for standard bath and pipette solutions. (**B**) Mean density of total (instantaneous plus time-dependent) inward and outward ROS-induced currents, measured at -160 mV and +100 mV, respectively, after 40 min treatment in a standard bath solution. Data are mean ± SE, n=18 and 15 for elongation and mature zones, respectively.

dependent current could not be defined unequivocally; instantaneous currents reversed around -30 mV, i.e. between equilibrium potentials for K^+ and Cl^-, supporting previous observations of its non-selective nature in accordance with Velarde-Buendía et al., (2012). Both

237 instantaneous and time-dependent $OH^{\bullet}$ -induced currents were significantly higher in the
238 apical zone. Total (instantaneous plus time-dependent) outward K^+ current was ~3-fold
239 higher in the root apex compared to the mature zone (Fig. 6 B). Surprisingly, addition of 80
240 mM NaCl had either no or little effect on the magnitude of $OH^{\bullet}$ -induced currents and reversal
241 potential of the instantaneous current (Fig. 6A). This implies: (1) a low discrimination
242 between Na^+ and Cl^- of the instantaneous current and (2) that its conductance was already
243 saturated at lower saline. Thus, any difference in the NSCC amplitude, observed between
244 apex and mature root zones more likely should be attributed to a difference in the surface
245 expression of ROS-activated ion transporters rather than their differential sensitivity to ROS.
246
247 ***Root metabolites are altered in the root apex after salinity stress***
248 Using GC-MS 75 metabolites in both apical and mature root zones were semi-quantified
249 before and after salinity stress; only statistically significant (Student's t-test p-value <0.05)
250 metabolite changes will be discussed (Table 1). Root treatment with 100 mM NaCl for 24 h
251 increased (2 to 5 fold) the content of 10 (out of 25 detected) amino acids in the root apex
252 (Table 1). By contrast, no changes were reported in the root amino acid profile in the mature
253 zone. The root apex also displayed a significant increase of 7 (out of 16) organic acids, with
254 particularly high fold changes detected for citrate and malate (16- and 27-fold, respectively),
255 and allantoin (6.7-fold). None of these changes were detected in the mature root zone. The
256 metabolite profile of the apical tissue also showed a strong decrease in the level of sugars and
257 sugar derivatives (5 of 13 analysed compounds); but with the exception of fructose, none of
258 these changes were significant in the mature zone (Table 1). Overall, out of 75 analysed
259 metabolites, significant changes were detected for 30 in the apical tissue, but only for 4 in the
260 mature root zone.
261
262 ***Exogenous application of allantoin reduced the extent of ROS-induced K^+ loss from barley***
263 ***roots***
264 As shown in Table 1, one of the most pronounced metabolic alterations observed in stressed
265 roots was a very significant (6-fold) increase in the level allantoin in the root apex. Given the
266 recent reports for the mitigating role of allantoin in oxidative stress damage in plants
267 (Watanabe et al., 2014), we tested effects of exogenously supplied allantoin on root ion flux
268 responses to ROS. Root pre-treatment with physiologically-relevant (1 mM) concentration of
269 allantoin has reduced the sensitivity of root apex to both salinity and ROS stresses (Fig 7).

The peak net K^+ efflux was reduced about 2 fold in allantoin-treated roots exposed to H_2O_2 Fig 7

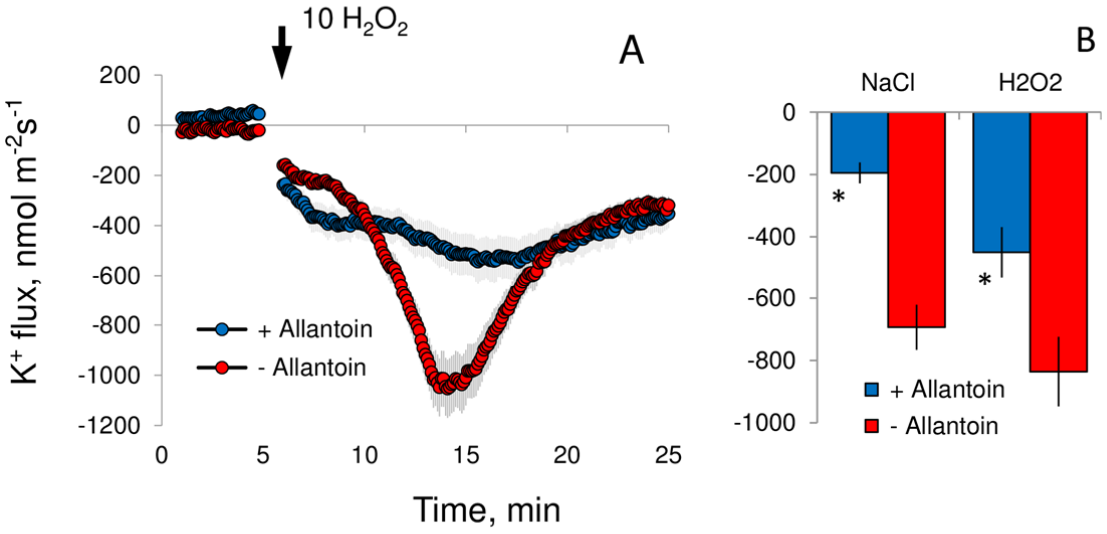

Fig 7: Effect of root pretreatment in 1 mM allantoin (for 24 h) on K^+ flux responses measured from epidermal root cells in the elongation zone upon exposure to salinity and oxidative stresses. **A** – transient net K^+ flux kinetics in response to 10 mM H_2O_2. **B** - peak K^+ flux values caused by acute salinity (100 mM NaCl) and oxidative (10 mM H_2O_2) stresses. Mean ± SE (n = 5 to 6). *Significant compared to non-pretreated control at $P < 0.05$.

stress (Fig 7AB); this reduction was 3-fold in case of roots treated with 100 mM NaCl (Fig 7B).

DISCUSSION

To assist in the interpretation of a complex dataset that highlights the importance of tissue-specific responses to salt treatment we have provided a model to explain the differential sensitivities between the apical and mature root tissues at the molecular level (see Fig 8).

Compromised K^+ retention but not differences in Na^+ accumulation or exclusion ability confers higher salt sensitivity to the root apex

Retention of stable K^+ concentrations in the cytosol is required to balance the toxic effects of Na^+ accumulation (Shabala and Pottosin, 2014; Anschutz et al., 2014). We demonstrate that the higher salt sensitivity of the root apex was not related to higher Na^+ accumulation in root tissues but rather originated from the compromised capacity for K^+ retention in the root apex.

A lower Na^+ accumulation in the root apex may be expected in the light of the predominant expression of SOS1 Na^+/H^+ exchangers in the root apex (Shi et al., 2000); hence the roots' Na^+ exclusion ability should be higher in this zone. Indeed, CoroNa Green fluorescence data suggests that under long-term salinity exposures root apical cells (and, specifically, cells in the elongation zone) accumulate less Na compared to those in the mature region of the root (Fig 2). Yet, despite this more pronounced Na^+ exclusion ability, root apical cells were much more sensitive to salinity, and root growth of the apex was completely arrested upon NaCl treatment (Fig 1).

Contrary to long-term trends, immediately upon salinity exposure net Na^+ influx was much higher in the apex (Fig. 2A). This could explain the ~40 mV difference in membrane depolarization between apical and mature root zones upon NaCl treatment (Fig. 3A), with major consequences to K^+ retention and cytosolic K^+ homeostasis (Fig. 3B), as NaCl-induced K^+ efflux in plant roots is mediated mainly by GORK channels which display very strong voltage dependency and are activated by membrane depolarization (see Fig 8; Anschutz et al., 2014).

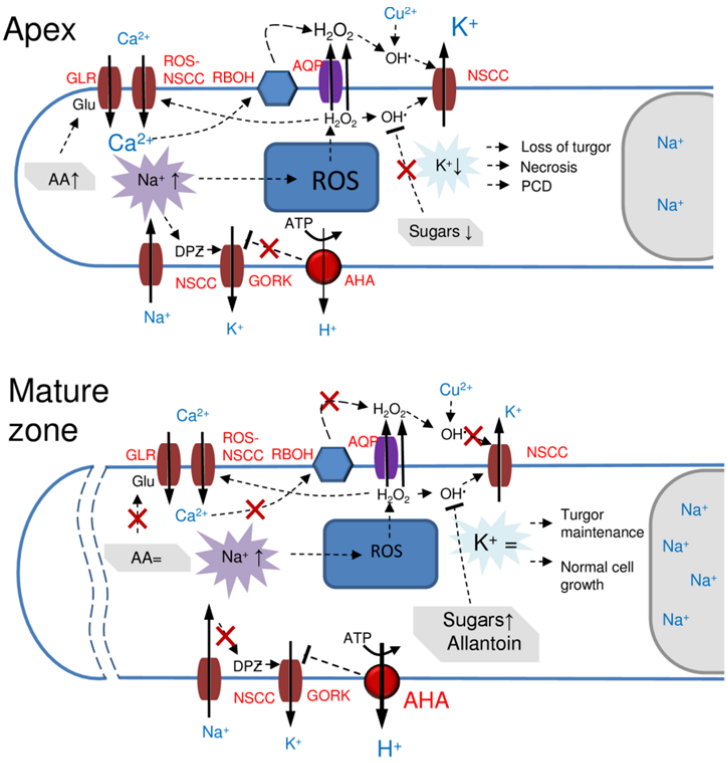

Fig 8: A model to explain differential sensitivity to salt stress between apical and mature root tissues. Abbreviations in red define specific plasma membrane (PM) transporters involved. NSCC, non-selective cation channel; GORK, outward-rectified depolarization-activated K^+ channel; APA, P_2B type H^+- ATPase; AQP, aquaporin; RBOH, NADPH oxidase; GLR, glutamate receptor channel; ROS-NSCC ROS-activated non-selective cation channel. **(A)** In the **root apex**, Na^+ transport across the PM is mediated by NSCC and results in a significant membrane depolarization (DPZ) leading to GORK activation and a massive efflux of K^+ from the cytosol. Increased Na^+ uptake also results in an increased ROS (H_2O_2) production in mitochondria. H_2O_2 then moves to the cytosol and is then transported to the apoplast (cell wall) either by diffusion or via AQP where it interacts with the transition metal (Cu^{2+} in the model), resulting in the formation of hydroxyl radicals ($OH^•$). The latter activates NSCC from the apoplastic side resulting in further K^+ loss from the cell. The cytosolic mode of NSCC activation by $OH^•$ is also possible. Elevation in cytosolic Na^+ also results in elevated cytosolic free Ca^{2+} pool stimulates RBOH activity, resulting in a further increase in H_2O_2 accumulation in the apoplast. Stress-induced increases in the amino acid pool (and, specifically, in glutamate (Glu)) stimulates additional Ca^{2+} uptake via GLR, leading to more H_2O_2 production by NADPH oxidase. The massive K^+ loss mediated by these three concurrent mechanisms results in the loss of the cell turgor (hence, root growth arrest) and, depending on severity of salt stress, either PCD or necrosis in the root apex. **(B)** In the **mature root zone**, intrinsically higher H^+-ATPase activity reduces the extent of DPZ and prevents activation of GORK. The observed increase in the sugar levels ensures efficient non-enzymatic scavenging of $OH^•$ thus preventing K^+ efflux via $OH^•$-activated NSCC. ROS-induced activation of K^+ efflux pathways is also prevented by allantoin. The constant level of the AA pool ensures the absence of activation of GLR and results in lesser formation of H_2O_2 by NADPH oxidase. Together with the higher vacuolar Na^+ content, these cells maintain normal turgor and metabolism and do not undergo PCD.

Cell elongation depends on the cell's ability to maintain turgor pressure and thus uptake of osmolytes and water by vacuoles. Sodium and potassium are two major inorganic osmolytes contributing up to 65% of cell turgor recovery in osmotically-stressed Arabidopsis roots (Shabala and Lew, 2002). In this study, the total sum of Na^+ and K^+ was not significantly different between the mature root zone and apex (Fig. 1E). Thus, the difference in turgor may not be the cause of the arrested root growth (Fig. 1C, D) upon the "apical treatment". Thus, the difference in the K^+ retention between the two zones needs to affect the growth in a more specific manner. This is further supported by the stress-specificity of the observed effects, which were not present when isotonic mannitol concentrations were used (Fig. 1E). Mannitol treatment did not result in membrane depolarization but instead lead to a slight hyperpolarization of the PM (Shabala and Lew, 2002) and resulted in an increased net K^+ uptake in both Arabidopsis (Shabala and Lew, 2002) and barley (Chen et al., 2005) roots. Consequently, upon mannitol treatment no significant growth difference was observed between the apex and mature zone (Fig. 1C, D). The process of cell elongation is not just a mechanical expansion, but instead an orchestrated process involving cell wall weakening, synthesis of organelles and other cellular components. One may assume that the higher net K^+ efflux (Fig 3B) implies a lower cytosolic K^+ (see Shabala et al., 2006 for direct evidence in

Arabidopsis) which could alter some of these processes, hence affecting the overall growth rate. In the longer term, an imbalance between the root and shoot growth would affect the roots' ability to supply water and nutrients to match shoot demands, with the consequent growth and yield penalties.

Intrinsically higher H^+-ATPase activity is essential to confer higher salinity tissue tolerance in mature root zone

High cytosolic K^+ levels required to provide optimal conditions for cell metabolism are achieved primarily by the maintenance of a large (-120 to -180 mV) negative voltage difference across the PM (Shabala and Pottosin, 2014). This resting potential is set by the PM H^+-ATPase and is normally kept close to the equilibrium potential for K^+, E_K (Hirsch et al., 1998). Under salinity, the membrane depolarizes following the influx of positively charged Na^+ ions, which shifts membrane potential values above E_K and results in significant outward K^+ currents (Anschutz et al., 2014; Very et al., 2014). This shift also implies that K^+ uptake may occur via active transport only. Intrinsically higher H^+-ATPase activity is essential to prevent this shift and to fuel the active K^+ uptake via H^+-coupled co-transport. Strong positive correlation between H^+-ATPase activity and salinity stress tolerance has been reported for several species (Bose et al., 2015), including barley (Chen et al., 2007). Here we show that this can also explain differential K^+ retention (and overall salinity stress sensitivity) between apical and mature root tissues (Fig. 3).

Could ROS contribute to a poorer K^+ retention?

Salt-induced Na^+/K^+ exchange across the plasma membrane is mediated by GORK and NSCC (see Fig 8; Shabala and Pottosin, 2014). A large contribution of NSCC is confirmed by the fact that Gd^{3+}, a known blocker of NSCC, caused a 60% inhibition of NaCl-induced K^+ efflux (Suppl. Fig. 2). ROS (reflecting mainly, but not specifically H_2O_2 levels) production under salt stress was substantially higher in the elongation zone (Fig. 4). H_2O_2 from either side of the membrane will activate inward-rectifying NSCC, mediating Ca^{2+} influx in the root elongation zone (Demidchik et al., 2007). On the other hand, the highly reactive OH•, formed upon H_2O_2 reduction by Fe^{2+} or Cu^+ causes membrane depolarization and activation of GORK and a variety of non-selective conductances, culminating in a massive K^+ efflux (Demidchik et al., 2010; Shabala and Pottosin, 2014). The OH•-induced K^+ current was 3-fold higher in the protoplasts from the elongation zone (Fig. 6). Combined with a larger

depolarization (Fig. 3A) and, hence, higher driving force for K^+ efflux, this would contribute to an even higher potentiation of net K^+ efflux in this zone (Fig. 5A). The OH•-induced K^+ efflux in the root mature zone of barley varieties with contrasting salt sensitivities, was not significantly different. Yet, on the background of elevated external polyamines, OH•-induced K^+ efflux was greatly potentiated in salt-sensitive and to a much lesser extent in salt-tolerant varieties (Velarde-Buendía et al., 2012). Upon salt stress, polyamines could be exported to the apoplast and oxidized there, forming H_2O_2 by cell-wall associated amine oxidase (Rodriguez et al., 2009). However, H_2O_2 can also across the membrane, by free diffusion or via aquaporins (Verdoucq et al., 2014). Once occurring in the apoplast, it could be reduced by either Cu- (diamine oxidase) or Fe- (POX), containing centers to OH• (see Fig 8; Liszkay et al., 2004; Pottosin et al., 2014). On the other hand, Cu import by specific transporters increases the cytosolic OH•-generation and activation of NSCC, mediating K^+ release *in vivo* (Rodrigo-Moreno et al., 2013). Therefore, effects of ROS in membrane conductance are not only defined by tissue-specific expression of ROS-sensitive transporters, but are contextual and depend on the ROS interconversion and transport as well as interaction with other factors (e.g. polyamines) (see Fig 8). In case of the OH•, which activates a plethora of K^+ release channels, the comparative efficiency of either internal or external action sites would be also dependent on the OH• -scavenging activity, which is much higher in the cytosol than in the apoplast.

$OH^{\bullet}$ cannot be scavenged by enzymatic antioxidants and can be reduced only by non-enzymatic means, with sugars and sugar alcohols playing a pivotal role in non-enzymatic ROS scavenging (Keunen et al., 2013). Here (Table 1) we show that the sugar and sugar alcohol levels decreased dramatically in the apex but only fructose and galactinol were decreased in the mature zone tissues. This may suggest that the reported difference in ROS sensitivity between the two different tissue types may be partially explained by the difference in non-enzymatic $OH^{\bullet}$ scavenging potential.

Furthermore, various plants respond to environmental stresses by activating enzymes, resulting in increased levels of allantoin and allantoate (Sagi et al., 1998). Recently, constitutive accumulation of allantoin was shown to improve overall plant performance under stress by activating ABA signaling pathways (Wang et al., 2012), and exogenous application mitigated oxidative damage symptoms (Watanabe et al., 2014). Here, we show that pre-treating barley roots with physiologically relevant concentrations of exogenously applied allantoin desensitized the root apical tissues and increased their ability to retain K^+ upon both

384 salinity and ROS exposure (Fig 7). In this context, the increased levels of allantoin in the
385 ROS-sensitive root apical cells may be interpreted as the plant's attempt to prevent stress-
386 induced K^+ loss. This increase in allantoin is not required in the mature zone, where stress-
387 induced ROS production is not observed (Fig 4).
388
389 ***Changes in primary metabolism exacerbate differential K^+ retention between tissues***
390 Salt treatment caused a clear change of the level of sugars, tricarboxylic acid (TCA) cycle
391 metabolites, and amino acids in the root apex but not in mature tissue (Table 1). Elevated
392 amino acid levels are commonly associated with increased tissue damage caused by salinity
393 (Widodo et al., 2009) and protein degradation (Dubey and Rani, 1990) and are believed to be
394 a non-specific reaction to salt stress rather than a plant response associated with tolerance
395 (Hill et al., 2013). The largest amino acid increase was for ornithine (5.83 fold in the apex;
396 Table 1). Physiologically relevant concentrations of ornithine have been shown to result in an
397 increased stress-induced K^+ efflux from roots (Cuin and Shabala, 2007), which could explain
398 the poor K^+ retention ability in the root apex reported in this study.
399 We also detected a strong increase in glutamate (5.16-fold) and glycine (5.99-fold) levels
400 in the root apex. Plant glutamate receptor-like (GLR) genes are closely related to mammalian
401 ionotropic glutamate receptors (iGluRs) (Price et al., 2012), which operate as Glu- and Gly-
402 gated NSCCs that catalyse the uptake of K^+, Na^+, and Ca^{2+} into neurons (Sohn, 2013). Plant
403 GLRs were recently confirmed to be NSCC (Price et al., 2012; Forde, 2014). Activated by
404 glutamate, GLR may therefore mediate stress-induced Ca^{2+} uptake, with a consequent raise in
405 cytosolic Ca^{2+}, that in turn can activate the plasma membrane NADPH oxidase (Lecourieux et
406 al., 2002), leading to elevated H_2O_2 levels and a consequent formation of hydroxyl radical (as
407 discussed above), leading to a massive K^+ efflux via OH•-activated outward-rectified
408 (GORK) K^+ channels (Demidchik et al., 2010). Thus, the strong increase in glutamate levels
409 found in the root apex (Table 1) may be an additional factor exacerbating a stress-induced
410 decrease in the cytosolic K^+ pool in this zone, leading to activation of caspase-like enzymes
411 and finally PCD (Fig. 7). Ser, found to have increased (2.17-fold) in the root apex, is also
412 known to be capable of activating GLRs in plants (Stephens et al., 2008).

MATERIALS AND METHODS

Plant material and growth conditions

Barley seeds (*Hordeum vulgare* L. cv CM72) were obtained from the Australian Winter Cereals Collection. Seeds were surface sterilized with 1% HClO for 15 min and thoroughly rinsed with distilled water. Plants were grown hydroponically in aerated BSM (Basal Salts Medium) solution containing 0.5 mM KCl, 0.1 mM $CaCl_2$ and 1 mM NaCl (pH 5.9) in the dark at room temperature (24 ± 1 °C). Four-day-old seedlings, with 70 to 80 mm long roots, were used for laboratory experiments.

Growth experiments

Barley roots were immobilized in a multi-compartment 120 mL chamber made of a rectangular 120 x 120 mm Petri dish with built-in Perspex partitions (Suppl. Fig S1). Narrow grooves were cut into the partitions to align roots. Grooves were sealed with petroleum jelly preventing any solution mixing between compartments (validated using dyes; Suppl. Fig S1). Appropriate solutions were added to each of the four compartments (I-IV; Fig 1A), and root length was measured daily for the entire duration of the experiment (3-4 days). Three seminal roots from the same plant were placed in each groove, and their tips were aligned to protrude precisely at the same distance (5 mm) into compartment IV.

Tissue ion content analysis

Root samples were quickly rinsed with 10 mM $CaCl_2$ to remove apoplastic Na^+, blotted dry with the paper towels and dried at 65 °C in a Unitherm Dryer (Birmingham, UK) to constant weight. Samples were then grounded and digested in 10 mL 98% H2SO4 and 3 mL 30% H_2O_2 for 5 h. The digested samples were diluted with distilled water to the required volume and root Na^+ and K^+ contents were analysed using a flame photometer (Corning 410C, Essex, UK).

Non-invasive ion flux measurements

Net K^+, Ca^{2+} and Na^+ fluxes were measured from apical (~ 3 mm from the tip) and mature (~ 20 mm) root zones using non-invasive microelectrode ion flux estimation (MIFE; Univ. Tasmania, Hobart, Australia). Briefly, borosilicate glass capillaries (GC150-10; Clark Electrochemical instruments, Pangbourne, Berks, UK) were pulled using a vertical puller. The

pulled electrodes were then dried in an oven at 220ºC overnight and silanized with tributilchlorosilane (Cat. No 90796; Fluka, Busch, Switzerland). After drying and cooling, electrodes were back filled with back filling solutions (200 mM KCl for K^+; 500 mM NaCl for Na^+; and 500 mM $CaCl_2$ for Ca^{2+}). The tips of respective electrodes were front filled with commercially available selectophore cocktails (Cat. No 60031 for K+; Cat. No 21048 for Ca^{2+}; both from Sigma-Aldrich, St, Louis, MO). For Na^+ flux measurements, recently developed calixarene-based microelectrodes with superior Na^+ selectivity were used (Jayakannan et al., 2011). Electrodes were calibrated in sets of appropriate solutions (see Shabala et al., 2006) and then used for measurements. Only electrodes with a slope above 50 mV per decade and correlation >0.999 were used.

Ready-to-measure seedlings were taken from the growth containers and their roots immobilised in the measuring chamber and pre-conditioned in BSM for 30 min. The measuring chamber was mounted on a microscope stage and electrode tips were positioned 40 µm from the root surface, with their tips aligned and separated by several µm, using a 3D micro manipulator. During the measurements, a computer-controlled stepper motor moved electrodes in a slow (5 s) square-wave cycle between the two positions, close to (40 µm) and away from (120 µm) the root surface. Steady-state ion fluxes were then recorded over a period of 5 min. Then, an appropriate treatment was administered, kinetics of net ion fluxes recorded for further 60 min. Net ion fluxes were measured at two positions along the longitudinal root axes: at 2 mm (elongation zone; Fig 1A) and at ~ 15 mm (mature zone) form the root tip.

Patch-clamp experiments

Epidermal root protoplasts were isolated by enzymatic digestion in enzyme solution containing 2% (w/v) cellulose (Yakult Honsha), 1.2% (w/v) cellulysin (Biosciences Inc.), 0.1% (w/v) pectolyase, 0.1% (w/v) bovine serum albumin, 10 mM KCl, 10 mM $CaCl_2$, and 2 mM $MgCl_2$, pH 5.7 adjusted with 2 mM MES, with osmolality set hypertonic (780 mOsM, set with sorbitol) with respect to the cell sap. After half-an-hour incubation of root segments either from mature or distal elongation zone at 30°C on a 90 rpm rotary shaker, preparation was rinsed with the same solution without enzymes and placed in a measuring chamber filled with a hypotonic (380 mOsM) solution, containing 10 mM KCl, 2 mM $CaCl_2$, and 1 mM $MgCl_2$, pH 5.7. After removing of the root debris, released protoplasts were washed by a solution applied for patch-clamp assays (see below) and those attached for the bottom were

used for further experiments. Protoplasts with a whole cell capacitance 5 to 10 pF (of epidermal origin; see Chen et al., 2007 for justification) were used in experiments. Measurements were made by means of Axopatch 200A patch-clamp amplifier (Axon Instruments). Patch-pipette were pulled in several steps on a Flaming-Brown P-97 micropipette puller (Sutter Instruments CO) and fire-polished on an L/M CPZ-101 microforge (List-Medical), yielding final resistance in standard bath/pipette solutions of 5-8 MΩ. Protoplasts were patch-clamped within 15 min after their release, and a new batch of protoplasts was used in each experiment. Once stable and low-leak (R_{leak}>5 GΩ) whole cell recording was established for approximately 15 min, Cu/A mixture (0.3/1 mM) was added directly to the bath, to generate $OH^{\bullet}$. Pipette solution contained (in mM): 100 KOH- HEPES- (pH 7.4), 3 $MgCl_2$, and 0.8 $CaCl_2$, 2 K_2EGTA; bath solution contained (in mM): 5 KCl, 2 $CaCl_2$, 0.5 $MgCl_2$; 2 MES-KOH (pH 6.0) or the same plus 80 mM NaCl (at the end of treatment). All patch solutions were adjusted to 500-560 mOsm by variable additions of sorbitol.

Membrane potential measurements

Conventional microelectrode (GC 150F-10, Harvard Apparatus Ltd, Kent, UK) with a tip diameter of ~0.5 μm was filled with 0.5 M KCl and connected to a MIFE electrometer via an Ag-AgCl half-cell. The mounted electrode was then impaled into the external cortex cells in either apical or mature root zones. Resting membrane potential measurements were recorded for 1 min before administering the treatment, and the resulting change in transient membrane potential was continuously monitored for up to 30 min. At least 6 individual plants were measured for each zone/treatment.

Intracellular Na^+ distribution

Cytosolic and vacuolar Na^+ content in barley roots was quantified using the green fluorescent Na^+ dye CoroNa Green acetoxymethyl ester (Molecular Probes, USA) essentially as described in Wu et al (2015). In brief, the CoroNa Green indicator stock was added to 5 mL of measuring buffer (10 mM KCl, 5 mM Ca^{2+}-MES, pH 6.1) and diluted to a final concentration of 15 mM. Appropriate root segments were cut from the apical and mature root zones and incubated for 2h in the dark in a solution containing 20μM CoroNa Green. After incubation, the samples were rinse in a buffered MES solution and examined using confocal microscopy. Confocal imaging was performed using an upright Leica Laser Scanning Confocal

Microscope SP5 (Leica Microsystems, Germany) equipped with a 40× oil immersion objective. The excitation wavelength was set at 488 nm, and the emission was detected at 510-520 nm. Six to 8 roots from individual plants were used and a minimum of 2 images were taken for each root zone. On average, readings from between 70 and 300 cells were averaged and reported for each zone (shown in Fig. 2). For analysis, several lines were drawn across the so-called "region of interest" (ROI) in an appropriate root zone. Continuous fluorescence intensity distribution profiles (quantified in arbitrary units by LAS software) were then obtained and plotted in an Excel file. The mean fluorescence intensity values for cytosolic and vacuolar compartments were then calculated for each cell by attributing signal profiles to root morphology (visualized by light microscopy images). A special attention was paid to the fact that apical root cells may contain multiple vacuoles. The data was then averaged for all cells measured for the same treatment. The background signal was measured from the empty region and then subtracted from the readings, to obtain corrected fluorescence values.

Plasma membrane isolation and H^+ transport activity

Seven day old barley seedlings were treated with either salt (NaCl, 100 mM) or water (control) for 24 h. Root apical and mature segments were cut. PMs were purified by two-phase partitioning as described in our previous publications (Pottosin et al., 2014). Proton pumping was measured by the quenching of 9-amino-6-chloro-2-methoxyacridine fluorescence (ACMA) (Lund and Fuglsang, 2012). PMs containing the H^+-ATPase were incubated with ATP (3 mM), and proton pumping was activated by addition of magnesium in roots treated with 100 mM NaCl for 24 h as compared with control roots. 10 μg PM protein was used for each analysis. The initial decrease in fluorescence after addition of Mg^{2+} was a direct effect of the amount of protons transported into the vesicles by the H^+-ATPase.

ROS detection

Apical (10 mm) and mature root sections were washed in 10 mM Tris-HCl buffer, incubated for 30 min at 37° with 25 μM 2',7'Dichlorofluorescein diacetate (DCF-DA, D6883, Sigma) assayed as described in Rodrigo-Moreno et al. (2013). ROS levels (in arbitrary units) were measured with the software Image-Pro Plus 6.0 (Media cybernetics Inc. Rockville, MD, USA).

Metabolite extraction, derivatisation, and GC-MS analysis

Five mm-long roots segments were isolated from apical and mature zones and approximately 20mg of each tissue (exact fresh weight recorded) was transferred into pre-chilled cryomill tubes (2ml 1.4mm-CK14 Ceramic bead kit, Sapphire Bioscience) and rapidly frozen in liquid nitrogen. 100µl of 100% methanol was added to the root tissue, containing 5µl of internal standard solution (1mg/ml $^{13}C_6$-sorbitol and L-$^{13}C_5$ ^{15}N-valine). The tissue in the solution was homogenised using an automatic mill (Precellys® 24) running at 6,400rpm for 30sec followed by an incubation at 70^{o}C for 15min. A further 100µl of water was added to root extracts. After centrifugation at 13,000rpm, an aliquot of 60µl of the extract was taken and dried *in vacuo* for subsequent derivatisation with *N*-Methyl-*N*-(tert-butyldimethylsilyl)trifluoro acetamide + 1% tert-butyldimethyl chlorosilane (TBS). An second aliquot of 70µl of the extracts was taken and dried *in vacuo* for subsequent derivatisation with *N*,*O*-*bis*(trimethylsilyl)trifluoroacetamide with 1% trimethylchlorosilane (TMS) (Sigma-Aldrich, Castle Hill, Australia). The dried extracts were re-dissolved and derivatised prior to injection using a Gerstel 2.5.2 autosampler (Gerstel, Mellinghofen, Germany) for 120 min at 37°C (10 µl of 30 mg/ml methoxyamine hydrochloride in pyridine) followed by treatment with 20 µl of TMS or 20µl TBS, and 2 µl of a retention time standard mixture (0.029% (v/v) *n*-dodecane, *n*-pentadecane, *n*-nonadecane, *n*-docosane, *n*-octacosane, *n*-dotriacontane and *n*-hexatriacontane dissolved in pyridine, all Sigma-Aldrich, Castle Hill, Australia) for another 30 min at 37°C. GC-MS data acquisition and data analysis was carried out exactly as described earlier (Hill et al., 2013).

Acknowledgement

We are thankful to Anette Lund for technical help.

Author Contributions

S.S. conceived the general concept and research plan; U.R., M.X., A.B, A.T.F, S.M. and C.P. supervised the experiments; L.S., S.S., J.Z., J.B., I.P. M.Z., A.V.B., C.P., A.M., H.W. and E.A. conducted experiments; S.S., I.P., C.B.H., A.T.F. and U.R. critically assessed the data; S.S. wrote the article; I.P., C.B.H., U.R., A.T.F. and A.B. have provided a critical assessment of the paper.

575 **Table 1**: Tissue-specific changes in the metabolite profile of barley roots in response to 100
576 mM NaCl treatment. Only metabolites showing significant (at $P < 0.05$) changes in one
577 of the zones are shown. Numbers shown in bold indicate significant ($P < 0.05$)
578 differences compared to the controls.
579

Metabolite	***Fold change***		***Metabolite***	***Fold change***	
	Mature	***Apex***		***Mature***	***Apex***
INCREASED (Apex)			**DECREASED (Apex)**		
Amino acids			*Amino acids*		
Aspartate	1.46	**2.75**	Leucine	**-2.04**	**-2.08**
Asparagine	-1.61	**4.3**	Tryptophan	**-5.88**	**-2.22**
Glutamate	1.17	**5.16**	*Organic and fatty acids*		
Glycine	1.6	**5.99**	Erythronate	-1.85	**-1.61**
Histidine	-2.70	**2.76**	*Sugars and derivatives*		
Lysine	1.25	**5.15**	Fructose	**-12.5**	-4.0
Ornithine	3.05	**5.83**	Galactinol	-12.5	**-3.57**
Serine	1.90	**2.17**	Inositol	1.52	**-2.27**
Threonine	1.35	**4.05**	Threitol	-1.75	**-3.03**
			Glucose 6P	1.67	**-4.55**
Organic acids			Glucose	-1.79	**-6.67**
Citrate	2.44	**16.78**			
Ferulate	1.09	**6.36**	**MIXED RESPONSES**		
Fumarate	1.45	**2.70**	*Amino acids*		
			Phenylalanine	**2.54**	**-2.94**
Quinate	-1.85	**1.95**			
Threonate	-1.89	**1.97**			
Malate	-1.11	**27.48**			
Sugars and derivatives					
Sucrose	-1.09	**1.92**			
Glycerate	-1.37	**1.40**			
Other compounds					
Allantoin	1.33	**6.65**			
Ethanolamine	1.38	**3.27**			

580

Figure legends

Fig 1: Barley root growth and responses to salinity (100 mM NaCl) and isotonic mannitol treatment. A – A schematic diagram depicting the experimental design and root immobilization within a multi-compartment growth chamber (see Suppl Fig 1). Salt was added to compartments II (mature zone) and IV (root apex), respectively. B – anatomy of barley root apex depicting functionally different root zones (modified from Ryan et al., 2016 with permission from Oxford University Press). RC – root cap; M – meristem; EZ – elongation zone; MZ – mature zone. C - Root growth rate as a function of time after treatment. Mean ± SE (n = 8 to 12). D – Relative growth rate (GR; % of control); E – total root Na^+ and K^+ content after 3 days of 100 mM NaCl application to either apical or mature root zones. Mean ± SE (n = 5 to 8). Man, mannitol; (M), mature zone; (A), apex. Different lowercase letters indicate significant differences between treatments at $P < 0.05$.

Fig 2: Na^+ uptake and accumulation in barley roots. **A** – kinetics of net Na^+ fluxes measured from the epidermal root cells in the apical and mature region in response to 100 mM NaCl treatment (indicated by an arrow). Mean ± SE (n = 6 to 8). **B, D**– Na^+ accumulation and intracellular distribution in mature (**B**) and apical (**D**) root zones visualized by the CoroNa Green fluorescence dye after 3 days of 100 mM NaCl treatment. One (of 8) typical image for each zone is shown. All images were taken using the same settings and exposure times to enable direct comparisons. Panels **C** and **E** show bright-field images of the corresponding zones for **B** and **D**, respectively. **F** – Mean CoroNa Green fluorescence intensity measured from cytosolic and vacuolar compartments. Mean ± SE (n = 70 to 300). Asterisk indicates significant differences between zones at $P < 0.05$. **G, H** – typical examples of the spatial cross-sectional profiles of CoroNa Green fluorescent signals from roots in apical and mature root zones, respectively. Several lines have been drawn across the so-called "region of interest" (ROI) in an appropriate root zone and continuous fluorescence intensity distribution profiles were obtained by LAS software and plotted. The scale bar in B-D is 25 μm.

Fig 3: Superior K^+ retention in the mature root zone is attributed to an intrinsically higher rate of H^+-ATPase extrusion activity. **A** – Changes in the PM potential in epidermal root cells in two different zones upon exposure to 100 mM NaCl. Mean ± SE (n = 6 to 8). **B** – Net K^+ fluxes measured from the epidermal root cells in the apical and mature zones in response to 100 mM NaCl treatment (indicated by an arrow). Mean ± SE (n = 7 to 10). **C**- H^+ pumping measured by ACMA quenching. PMs containing the H^+-ATPase were

614 incubated with ATP, and H^+ pumping was activated by addition of Mg^{2+} (indicated by an
615 arrow). The experiment is a representative of three independent PM purifications.
616 **Fig 4:** Stress-induced ROS accumulation in barley roots visualised by 2', 7'
617 Dichlorofluorescein diacetate (DCF-DA) staining (see Rodrigo-Moreno et al., 2013 for
618 details). Panels **A** to **D** show representative (one of eight) images of mature (~20 mm from
619 tip) and apical (2 mm) zones from control and salt-treated (100 mM NaCl for 24 h) roots.
620 **E** - average fluorescence signal intensity from the midst of the apical and mature root zone
621 (in arbitrary units) for control and stressed roots. Mean ± SE (n = 8). **F** – as above, for root
622 treated with isotonic mannitol solution. Data labelled with different lower case letters is
623 significantly different at $P < 0.05$. The scale bar in panels A-D is 200 μm.
624 **Fig 5**: Net K^+ (A) and Ca^{2+} (B) fluxes measured from epidermal root cells in response to $OH^{\bullet}$-
625 generating Cu/ascorbate (0.3/1 mM) mix applied at 5 min (as indicated by an arrow). Mean
626 ± SE (n = 6 to 8).
627 **Fig 6:** ROS induced non-selective current in protoplasts from elongation and mature root
628 zones. (A) Examples of whole cell recordings of membrane currents, induced by OH• in
629 two protoplasts of equal size (C=5.5 pF), isolated from mature or elongation root zones.
630 Ionic concentrations are given in Materials and Methods. Respective I/V curves for
631 instantaneous and time-dependent current components at the beginning of treatment (2
632 min), 40 min after, and after a subsequent addition of 80 mM NaCl are presented. Arrows
633 indicate equilibrium potentials for K^+ and Cl^- for standard bath and pipette solutions. (B)
634 Mean density of total (instantaneous plus time-dependent) inward and outward ROS-
635 induced currents, measured at -160 mV and +100 mV, respectively, after 40 min treatment
636 in a standard bath solution. Data are mean ± SE, n=18 and 15 for elongation and mature
637 zones, respectively.
638 **Fig 7:** Effect of root pretreatment in 1 mM allantoin (for 24 h) on K^+ flux responses measured
639 from epidermal root cells in the elongation zone upon exposure to salinity and oxidative
640 stresses. **A** – transient net K^+ flux kinetics in response to 10 mM H_2O_2. **B** - peak K^+ flux
641 values caused by acute salinity (100 mM NaCl) and oxidative (10 mM H_2O_2) stresses.
642 Mean ± SE (n = 5 to 6). *Significant compared to non-pretreated control at $P < 0.05$.
643 **Fig 8**: A model to explain differential sensitivity to salt stress between apical and mature root
644 tissues. Abbreviations in red define specific plasma membrane (PM) transporters involved.
645 NSCC, non-selective cation channel; GORK, outward-rectified depolarization-activated K^+
646 channel; APA, P_2B type H^+- ATPase; AQP, aquaporin; RBOH, NADPH oxidase; GLR,

647 glutamate receptor channel; ROS-NSCC, ROS-activated non-selective cation channel. **(A)**
648 In the **root apex**, Na^+ transport across the PM is mediated by NSCC and results in a
649 significant membrane depolarization (DPZ) leading to GORK activation and a massive
650 efflux of K^+ from the cytosol. Increased Na^+ uptake also results in an increased ROS
651 (H_2O_2) production in mitochondria. H_2O_2 then moves to the cytosol and is then transported
652 to the apoplast (cell wall) either by diffusion or via AQP where it interacts with the
653 transition metal (Cu^{2+} in the model), resulting in the formation of hydroxyl radicals ($OH^{\bullet}$).
654 The latter activates NSCC from the apoplastic side resulting in further K^+ loss from the
655 cell. The cytosolic mode of NSCC activation by $OH^{\bullet}$ is also possible. Elevation in
656 cytosolic Na^+ also results in elevated cytosolic free Ca^{2+} pool stimulates RBOH activity,
657 resulting in a further increase in H_2O_2 accumulation in the apoplast. Stress-induced
658 increases in the amino acid pool (and, specifically, in glutamate (Glu)) stimulates
659 additional Ca^{2+} uptake via GLR, leading to more H_2O_2 production by NADPH oxidase.
660 The massive K^+ loss mediated by these three concurrent mechanisms results in the loss of
661 the cell turgor (hence, root growth arrest) and, depending on severity of salt stress, either
662 PCD or necrosis in the root apex. **(B)** In the **mature root zone**, intrinsically higher H^+-
663 ATPase activity reduces the extent of DPZ and prevents activation of GORK. The
664 observed increase in the sugar levels ensures efficient non-enzymatic scavenging of $OH^{\bullet}$
665 thus preventing K^+ efflux via $OH^{\bullet}$-activated NSCC. ROS-induced activation of K^+ efflux
666 pathways is also prevented by allantoin. The constant level of the AA pool ensures the
667 absence of activation of GLR and results in lesser formation of H_2O_2 by NADPH oxidase.
668 Together with the higher vacuolar Na^+ content, these cells maintain normal turgor and
669 metabolism and do not undergo PCD.
670
671
672

Parsed Citations

Adem GD, Roy SJ, Zhou M, Bowman JP, Shabala S (2014) Evaluating contribution of ionic, osmotic and oxidative stress components towards salinity tolerance in barley. BMC Plant Biol 14: 113.
Pubmed: Author and Title
CrossRef: Author and Title
Google Scholar: Author Only Title Only Author and Title

Anschütz U, Becker D, Shabala S (2014) Going beyond nutrition: Regulation of potassium homoeostasis as a common denominator of plant adaptive responses to environment. J Plant Physiol 171: 670-687.
Pubmed: Author and Title
CrossRef: Author and Title
Google Scholar: Author Only Title Only Author and Title

Bose J, Rodrigo-Moreno A, Lai DW, Xie YJ, Shen WB, Shabala S (2015) Rapid regulation of the plasma membrane H+-ATPase activity is essential to salinity tolerance in two halophyte species, Atriplex lentiformis and Chenopodium quinoa. Ann Bot 115: 481-494.
Pubmed: Author and Title
CrossRef: Author and Title
Google Scholar: Author Only Title Only Author and Title

Chen Z, Newman I, Zhou M, Mendham N, Zhang G, Shabala S (2005) Screening plants for salt tolerance by measuring K+ flux: a case study for barley. Plant Cell Environ 28: 1230-1246.
Pubmed: Author and Title
CrossRef: Author and Title
Google Scholar: Author Only Title Only Author and Title

Chen ZH, Pottosin, II, Cuin TA, Fuglsang AT, Tester M, Jha D, Zepeda-Jazo I, Zhou MX, Palmgren MG, Newman IA, Shabala S (2007) Root plasma membrane transporters controlling K+/Na+ homeostasis in salt-stressed barley. Plant Physiol 145: 1714-1725.
Pubmed: Author and Title
CrossRef: Author and Title
Google Scholar: Author Only Title Only Author and Title

Cuin TA, Shabala S (2007) Compatible solutes reduce ROS-induced potassium efflux in Arabidopsis roots. Plant Cell Environ 30: 875-885.
Pubmed: Author and Title
CrossRef: Author and Title
Google Scholar: Author Only Title Only Author and Title

Demidchik V (2015) Mechanisms of oxidative stress in plants: From classical chemistry to cell biology. Env Exp Bot 109: 212-228.
Pubmed: Author and Title
CrossRef: Author and Title
Google Scholar: Author Only Title Only Author and Title

Demidchik V, Cuin TA, Svistunenko D, Smith SJ, Miller AJ, Shabala S, Sokolik A, Yurin V (2010) Arabidopsis root K+-efflux conductance activated by hydroxyl radicals: single-channel properties, genetic basis and involvement in stress-induced cell death. J Cell Sci 123: 1468-1479.
Pubmed: Author and Title
CrossRef: Author and Title
Google Scholar: Author Only Title Only Author and Title

Demidchik V, Maathuis FJM (2007) Physiological roles of nonselective cation channels in plants: from salt stress to signalling and development. New Phytol 175: 387-404.
Pubmed: Author and Title
CrossRef: Author and Title
Google Scholar: Author Only Title Only Author and Title

Demidchik V, Straltcova D, Medvedev SS, Pozhvanov GA, Sokolik A, Yurin V (2014) Stress-induced electrolyte leakage: the role of K+ channels and involvement in programmed cell death and metabolic adjustment. J Exp Bot 65: 1259-1270.
Pubmed: Author and Title
CrossRef: Author and Title
Google Scholar: Author Only Title Only Author and Title

Demidchik V, Shabala SN, Davies JM (2007) Spatial variation in H2O2 response of Arabidopsis thaliana root epidermal Ca2+ flux and plasma membrane Ca2+ channels. Plant J 49: 377-386.
Pubmed: Author and Title
CrossRef: Author and Title
Google Scholar: Author Only Title Only Author and Title

Dinneny JR (2010) Analysis of the salt-stress response at cell-type resolution. Plant Cell Environ 33: 543-551.
Pubmed: Author and Title
CrossRef: Author and Title
Google Scholar: Author Only Title Only Author and Title

Dinneny JR, Long TA, Wang JY, Jung JW, Mace D, Pointer S, Barron C, Brady SM, Schiefelbein J, Benfey PN (2008) Cell identity mediates the response of Arabidopsis roots to abiotic stress. Science 320: 942-945.
Pubmed: Author and Title
CrossRef: Author and Title
Google Scholar: Author Only Title Only Author and Title

Dubey RS, Rani M (1990) Influence of NaCl salinity on the behavior of protease, aminopeptidase and carboxypeptidase in rice seedlings in relation to salt tolerance. Aust J Plant Physiol 17: 215-221.
Pubmed: Author and Title
CrossRef: Author and Title
Google Scholar: Author Only Title Only Author and Title

Flowers TJ (2004) Improving crop salt tolerance. J Exp Bot 55: 307-319.
Pubmed: Author and Title
CrossRef: Author and Title
Google Scholar: Author Only Title Only Author and Title

Flowers TJ, Munns R, Colmer TD (2015) Sodium chloride toxicity and the cellular basis of salt tolerance in halophytes. Ann Bot 115:419-431.
Pubmed: Author and Title
CrossRef: Author and Title
Google Scholar: Author Only Title Only Author and Title

Forde BG (2014) Glutamate signalling in roots. J Exp Bot 65: 779-787.
Pubmed: Author and Title
CrossRef: Author and Title
Google Scholar: Author Only Title Only Author and Title

Hill CB, Jha D, Bacic A, Tester M, Roessner U (2013) Characterization of ion contents and metabolic responses to salt stress of different Arabidopsis AtHKT1;1 genotypes and their parental strains. Mol Plant 6: 350-368.
Pubmed: Author and Title
CrossRef: Author and Title
Google Scholar: Author Only Title Only Author and Title

Hirsch RE, Lewis BD, Spalding EP, Sussman MR (1998) A role for the AKT1 potassium channel in plant nutrition. Science 280: 918-921.
Pubmed: Author and Title
CrossRef: Author and Title
Google Scholar: Author Only Title Only Author and Title

Jayakannan M, Babourina O, Rengel Z (2011) Improved measurements of Na+ fluxes in plants using calixarene-based microelectrodes. J Plant Physiol 168:1045-1051.
Pubmed: Author and Title
CrossRef: Author and Title
Google Scholar: Author Only Title Only Author and Title

Ji HT, Pardo JM, Batelli G, Van Oosten MJ, Bressan RA, Li X (2013) The Salt Overly Sensitive (SOS) pathway: established and emerging roles. Mol Plant 6:275-286.
Pubmed: Author and Title
CrossRef: Author and Title
Google Scholar: Author Only Title Only Author and Title

Julkowska MM, Testerink C (2015) Tuning plant signaling and growth to survive salt. Trends Plant Sci 20:586-594.
Pubmed: Author and Title
CrossRef: Author and Title
Google Scholar: Author Only Title Only Author and Title

Keunen E, Peshev D, Vangronsveld J, Van den Ende W, Cuypers A (2013) Plant sugars are crucial players in the oxidative challenge during abiotic stress: extending the traditional concept. Plant Cell Environ 36: 1242-1255.
Pubmed: Author and Title
CrossRef: Author and Title
Google Scholar: Author Only Title Only Author and Title

Kurusu T, Kuchitsu K, Tada Y (2015) Plant signaling networks involving Ca2+ and Rboh/Nox-mediated ROS production under salinity stress. Frontiers Plant Sci 6: 427.
Pubmed: Author and Title
CrossRef: Author and Title
Google Scholar: Author Only Title Only Author and Title

Lecourieux D, Mazars C, Pauly N, Ranjeva R, Pugin A (2002) Analysis and effects of cytosolic free calcium increases in response to elicitors in Nicotiana plumbaginifolia cells. Plant Cell 14: 2627-2641.
Pubmed: Author and Title
CrossRef: Author and Title
Google Scholar: Author Only Title Only Author and Title

Liszkay A, van der Zalm E, Schopfer P (2004). Production of reactive oxygen intermediates (-O2, H2O2 and -OH) by maize roots and their role in wall loosening and elongation growth. Plant Physiol 136: 3114-3123.
Pubmed: Author and Title
CrossRef: Author and Title
Google Scholar: Author Only Title Only Author and Title

Lund A, Fuglsang AT (2012) Purification of plant plasma membranes by two-phase partitioning and measurement of H+ pumping. Methods Mol Biol 913:217-23.
Pubmed: Author and Title
CrossRef: Author and Title
Google Scholar: Author Only Title Only Author and Title

Ma SS, Bohnert HJ (2007) Integration of Arabidopsis thaliana stress-related transcript profiles, promoter structures, and cell-specific expression. Genome Biol 8: R49.
Pubmed: Author and Title
CrossRef: Author and Title
Google Scholar: Author Only Title Only Author and Title

Ma SS, Gong QQ, Bohnert HJ (2006) Dissecting salt stress pathways. J Exp Bot 57:1097-1107.
Pubmed: Author and Title
CrossRef: Author and Title
Google Scholar: Author Only Title Only Author and Title

Mittler R (2002) Oxidative stress, antioxidants and stress tolerance. Trends Plant Sci 7: 405-410.
Pubmed: Author and Title
CrossRef: Author and Title
Google Scholar: Author Only Title Only Author and Title

Palmgren MG, Nissen P (2011) P-Type ATPases. Annu Rev Biophys 40: 243-266.
Pubmed: Author and Title
CrossRef: Author and Title
Google Scholar: Author Only Title Only Author and Title

Pottosin I, Velarde-Buendía AM, Bose J, Fuglsang AT, Shabala S (2014) Polyamines cause plasma membrane depolarization, activate Ca-, and modulate H-ATPase pump activity in pea roots. J Exp Bot 65: 2463-2472.
Pubmed: Author and Title
CrossRef: Author and Title
Google Scholar: Author Only Title Only Author and Title

Price MB, Jelesko J, Okumoto S (2012) Glutamate receptor homologs in plants: functions and evolutionary origins. Front Plant Sci 3: 235.
Pubmed: Author and Title
CrossRef: Author and Title
Google Scholar: Author Only Title Only Author and Title

Qadir M, Quillérou E, Nangia V, Murtaza G, Singh M, Thomas RJ, Drechsel P, Noble AD (2014) Economics of salt-induced land degradation and restoration. Nat Res Forum DOI: 10.1111/1477-8947.12054
Pubmed: Author and Title
CrossRef: Author and Title
Google Scholar: Author Only Title Only Author and Title

Rodrigo-Moreno A, Andreas-Colas N, Poschenrieder C, Gunse B, Pellarrubia L, Shabala S (2013) Calcium- and potassium-permeable plasma membrane transporters are activated by copper in Arabidopsis root tips: Linking copper transport with cytosolic hydroxyl radical production. Plant Cell Environ 36: 844-855.
Pubmed: Author and Title
CrossRef: Author and Title
Google Scholar: Author Only Title Only Author and Title

Roy SJ, Negrao S, Tester M (2014) Salt resistant crop plants. Curr Opin Biotech 26:115-124.
Pubmed: Author and Title
CrossRef: Author and Title
Google Scholar: Author Only Title Only Author and Title

Rudashevskaya EL, Ye J, Jensen ON, Fuglsang AT, Palmgren MG (2012). Phosphosite mapping of P-type plasma membrane H+-ATPase in homologous and heterologous environments. J Biol Chem 287: 4904-4913.
Pubmed: Author and Title
CrossRef: Author and Title
Google Scholar: Author Only Title Only Author and Title

Sagi M, Omarov RT, Lips SH (1998) The Mo-hydroxylases xanthine dehydrogenase and aldehyde oxidase in ryegrass as affected by nitrogen and salinity. Plant Sci 135: 125-135.
Pubmed: Author and Title
CrossRef: Author and Title
Google Scholar: Author Only Title Only Author and Title

Shabala L, Cuin TA, Newman IA, Shabala S (2005) Salinity-induced ion flux patterns from the excised roots of Arabidopsis sos mutants. Planta 222: 1041-1050.
Pubmed: Author and Title
CrossRef: Author and Title
Google Scholar: Author Only Title Only Author and Title

Shabala L, Ross T, McMeekin T, Shabala S (2006) Non-invasive microelectrode ion flux measurements to study adaptive responses of microorganisms to the environment. FEMS Microb Rev 30: 472-486.
Pubmed: Author and Title
CrossRef: Author and Title
Google Scholar: Author Only Title Only Author and Title

Shabala S, Demidchik V, Shabala L, Cuin TA, Smith SJ, Miller AJ, Davies JM, Newman IA (2006) Extracellular Ca2+ ameliorates NaCl-induced K+ loss from Arabidopsis root and leaf cells by controlling plasma membrane K+-permeable channels. Plant Physiol 141: 1653-1665.
Pubmed: Author and Title
CrossRef: Author and Title
Google Scholar: Author Only Title Only Author and Title

Shabala S (2009) Salinity and programmed cell death: unravelling mechanisms for ion specific signalling. J Exp Bot 60: 709-711.
Pubmed: Author and Title
CrossRef: Author and Title
Google Scholar: Author Only Title Only Author and Title

Shabala S (2013) Learning from halophytes: physiological basis and strategies to improve abiotic stress tolerance in crops. Ann Bot 112: 1209-1221.
Pubmed: Author and Title
CrossRef: Author and Title
Google Scholar: Author Only Title Only Author and Title

Shabala S, Lew RR (2002) Turgor regulation in osmotically stressed Arabidopsis epidermal root cells. Direct support for the role of inorganic ion uptake as revealed by concurrent flux and cell turgor measurements. Plant Physiol 129: 290-299.
Pubmed: Author and Title
CrossRef: Author and Title
Google Scholar: Author Only Title Only Author and Title

Shabala S, Pottosin I (2014) Regulation of potassium transport in plants under hostile conditions: implications for abiotic and biotic stress tolerance. Physiol Plant 151: 257-279.
Pubmed: Author and Title
CrossRef: Author and Title
Google Scholar: Author Only Title Only Author and Title

Shi HZ, Ishitani M, Kim CS, Zhu JK (2000) The Arabidopsis thaliana salt tolerance gene SOS1 encodes a putative Na+/H+ antiporter. Proc Natl Acad Sci USA 97: 6896-6901.
Pubmed: Author and Title
CrossRef: Author and Title
Google Scholar: Author Only Title Only Author and Title

Shi HZ, Quintero FJ, Pardo JM, Zhu JK (2002) The putative plasma membrane Na+/H+ antiporter SOS1 controls long-distance Na+ transport in plants. Plant Cell 14: 465-477.
Pubmed: Author and Title
CrossRef: Author and Title
Google Scholar: Author Only Title Only Author and Title

Sohn JW (2013) Ion channels in the central regulation of energy and glucose homeostasis. Frontiers Neurosci 7: 85.
Pubmed: Author and Title
CrossRef: Author and Title
Google Scholar: Author Only Title Only Author and Title

Stephens NR, Qi Z, Spalding EP (2008) Glutamate receptor subtypes evidenced by differences in desensitization and dependence on the GLR3.3 and GLR3.4 genes. Plant Physiol 146: 529-538.
Pubmed: Author and Title
CrossRef: Author and Title
Google Scholar: Author Only Title Only Author and Title

Sun Y, Kong X, Li C, Liu Y, Ding Z (2015) Potassium retention under salt stress is associated with natural variation in salinity tolerance among Arabidopsis accessions. PLOS One 10(5): e0124032.
Pubmed: Author and Title
CrossRef: Author and Title
Google Scholar: Author Only Title Only Author and Title

Tester M, Davenport R (2003) Na+ tolerance and Na+ transport in higher plants. Ann Bot 91: 503-527.
Pubmed: Author and Title
CrossRef: Author and Title
Google Scholar: Author Only Title Only Author and Title

Velarde-Buendia AM, Shabala S, Cvikrova M, Dobrovinskaya O, Pottosin I (2012) Salt-sensitive and salt-tolerant barley varieties differ in the extent of potentiation of the ROS-induced K+ efflux by polyamines. Plant Physiol Biochem 61:18-23.
Pubmed: Author and Title
CrossRef: Author and Title
Google Scholar: Author Only Title Only Author and Title

Very AA, Nieves-Cordones M, Daly M, Khan I, Fizames C, Sentenac H (2014) Molecular biology of K+ transport across the plant cell membrane: what do we learn from comparison between plant species? J Plant Physiol 171: 748-769.
Pubmed: Author and Title
CrossRef: Author and Title
Google Scholar: Author Only Title Only Author and Title

Verdoucq L, Rodrigues O, Martiniere A, Luu DT, Maurel C (2014) Plant aquaporins on the move: reversible phosphorylation, lateral motion and cycling. Curr Opin Plant Biol 22:101-107.
Pubmed: Author and Title
CrossRef: Author and Title
Google Scholar: Author Only Title Only Author and Title

Wang P, Kong CH, Sun B, Xu XH (2012) Distribution and function of allantoin (5-ureidohydantoin) in rice grains. J Agric Food Chem 60: 2793-2798.
Pubmed: Author and Title
CrossRef: Author and Title
Google Scholar: Author Only Title Only Author and Title

Watanabe S, Matsumoto M, Hakomori Y, Takagi H, Shimada H, Sakamoto A (2014) The purine metabolite allantoin enhances abiotic stress tolerance through synergistic activation of abscisic acid metabolism. Plant Cell Environ 37: 1022-1036.
Pubmed: Author and Title
CrossRef: Author and Title
Google Scholar: Author Only Title Only Author and Title

Widodo, Patterson JH, Newbigin E, Tester M, Bacic A, Roessner U (2009) Metabolic responses to salt stress of barley (Hordeum vulgare L.) cultivars, Sahara and Clipper, which differ in salinity tolerance. J Exp Bot 60: 4089-4103.
Pubmed: Author and Title
CrossRef: Author and Title
Google Scholar: Author Only Title Only Author and Title

Wu HH, Shabala L, Liu XH, Azzarello E, Zhou M, Pandolfi C, Chen ZH, Bose J, Mancuso S, Shabala S (2015) Linking salinity stress tolerance tissue-specific Na+ sequestration in wheat roots. Frontiers Plant Sci 6; doi:10.3389/fpls.2015.00071
Pubmed: Author and Title
CrossRef: Author and Title
Google Scholar: Author Only Title Only Author and Title

Wu JL, Seliskar DM (1998) Salinity adaptation of plasma membrane H+-ATPase in the salt marsh plant Spartina patens: ATP hydrolysis and enzyme kinetics. J Exp Bot 49: 1005-1013.
Pubmed: Author and Title
CrossRef: Author and Title
Google Scholar: Author Only Title Only Author and Title